Influence of a resonant surface nonlinearity on the scattering of light from a randomly rough surface

Tamara A. Leskova
Institute of Spectroscopy, Russian Academy of Sciences, Troitsk 142092, Russia

Alexei A. Maradudin and Andrei V. Shchegrov
Department of Physics and Astronomy and Institute for Surface and Interface Science, University of California, Irvine, California 92697

(Received 23 December 1997)

We study the scattering of light from a one-dimensional, randomly rough surface of a linear dielectric coated by a thin resonantly nonlinear film. We focus on the coherent scattering phenomena occurring at the frequency of the incident light and show that the scattering properties of this system can be described by a single, nonlinear, impedance boundary condition. We obtain thereby a nonlinear integral equation for the electric field on the surface and present algorithms for its numerical solution in different scattering regimes. We investigate the effect of nonlinearity on enhanced backscattering from this system, and the effect of random surface roughness on optical bistability in reflection. [S1063-651X(98)02206-5]

PACS number(s): 42.25.Fx, 42.65.Pc, 68.35.Ct

I. INTRODUCTION

Theoretical and experimental investigations of multiple-scattering effects in the interaction of light with disordered nonlinear volume media have been intensively carried out for the past decade. They centered on the enhanced backscattering effect for second-harmonic light scattered from a disordered dielectric slab [1,2], difference frequency parametric mixing of two light beams in a disordered nonlinear medium [3], angular intensity correlation function for second-harmonic light generated inside a random dielectric waveguide [4], and some other related phenomena.

Disordered nonlinear surface systems, like their volume counterparts, have also attracted a good deal of attention and have proved to manifest coherent multiple-scattering phenomena. Thus McGurn *et al.* [5] used a perturbative approach to predict enhanced second-harmonic generation of light at a weakly rough, clean metal surface that occurs not only in the retroreflection direction but also in the direction normal to the mean scattering surface. The multiple scattering of surface plasmon polaritons, excited by the incident light on the rough vacuum-metal interface, plays the decisive role in the appearance of both peaks in this theory. This work stimulated several experimental studies of second-harmonic generation in the multiple scattering of light from metal surfaces [6–10], in which, however, the scattering system was not a clean random interface between vacuum and a semi-infinite metal but the random interface with vacuum of a thin metal film deposited on the planar base of a dielectric prism through which the light was incident (the Kretschmann attenuated total reflection geometry). The first experimental studies of multiple-scattering effects in the second-harmonic generation of light scattered from a clean one-dimensional vacuum-metal interface were carried out in a series of papers by O'Donnell and his colleagues [11–13], in which it was found that for both weakly and strongly rough surfaces a dip is present in the retroreflection direction in the angular dependence of the intensity of the scattered second-harmonic light rather than the peak that occurs in scattering at the fundamental frequency. This result was in agreement with the rigorous numerical simulation results of second-harmonic generation from such surfaces carried out by Leyva-Lucero *et al.* [14].

Thus the overwhelming majority of investigations on light scattering from nonlinear disordered volumes or surfaces concentrated on the multiple-scattering phenomena that occur at the generated frequencies (primarily, second harmonic). In many nonlinear media (e.g., Kerr media), however, the strongest nonlinear effects occur at the frequency of the incident light. The lack of any quantitative theoretical results on the multiple scattering of light from such media is caused primarily by the complexity of the theory, even in the absence of disorder. Nevertheless, efforts in this direction are expected to be rewarding, since such systems exhibit diverse and intense physical phenomena even in the absence of disorder (e.g., optical bistability), and in the absence of nonlinearity (e.g., the enhanced backscattering effect). Such nonlinear effects as the switching of the interface from one at which total internal reflection occurs to one that transmits light through it as the intensity of the incident light is increased, and bistable reflection of light from it, were predicted and subsequently observed experimentally [15]. It is of considerable practical importance to know how the randomness of the interface affects these and other nonlinear effects occurring at it. A somewhat qualitative discussion of this question has been presented recently by Bass and Freilikher [16], but with no quantitative results. Another question of interest is how nonlinearity affects the enhanced backscattering of light from a random surface.

In this paper we study quantitatively the scattering of *s*-polarized light from the one-dimensional random surface of a semi-infinite linear dielectric medium on which a thin nonlinear semiconducting film of constant thickness is deposited. The frequency of the incident light is assumed to be close to that of the excitonic resonance in the film, so that the reflecting and absorbing properties of the surface are very sensitive to the intensity of the incident electromagnetic field and to the resulting field distribution on the rough vacuum-

(nonlinear) dielectric interface. This nonlinear, thin film system was chosen because (i) it is experimentally realizable, (ii) the equations that have to be solved can be reduced to a tractable form in this case, (iii) nonlinear planar layered systems are known [17] to display the effect of optical bistability in the reflection of light, and (iv) rough film systems provide an additional degree of freedom compared to systems with a single rough interface, and therefore allow easier manipulating with parameters of the system to achieve desired scattering characteristics or even produce new coherent scattering phenomena [18–20].

Finally, there is a methodological consideration prompting this work. In a rigorous computer simulation study of the scattering light from, and its transmission through, a linear film with one-dimensional random surfaces, the application of Green's second integral identity in the plane [21] yields the result that the value of the electromagnetic field at any point in space is given in terms of integrals along the curve bounding the film. In contrast, when the film is characterized by a nonlinear dielectric function instead of by a linear one, these line integrals are supplemented by an integral taken throughout the area bounded by the curves along which the line integrals are evaluated, in which the field being sought enters the integrand nonlinearly. The result is a very computationally intense problem. In the present case we overcome this problem, at least in part, by assuming that the thickness of the nonlinear film is small compared to the wavelength of the incident light, and using an impedance boundary condition at the interface between the nonlinear film and the linear substrate, to derive an effective, nonlinear, boundary condition that the electromagnetic field in the vacuum region satisfies on the surface of the substrate. In this way we obtain a single, one-dimensional, nonlinear integral equation for the value of the electric field on the surface, which is solved numerically for a given value of the intensity of the incident field. The angular dependence of the intensity of the coherent and incoherent components of the scattered light are obtained by repeating this calculation for a large number of realizations of the random surface profile and averaging the results over this ensemble. This program is carried out for each of a set of values of the intensity of the incident field. It is hoped that this approach will be useful in the solution of a variety of scattering problems in which the scattering system is a thin nonlinear film with one or two random surfaces.

The outline of this paper is the following. In Sec. II we describe the scattering system and write the basic equations and the boundary conditions for the electric field. We then specify the form of the incident field and define the characteristics of the scattered intensity we are going to calculate. In Sec. III we derive the effective nonlinear boundary condition for the electric field in the vacuum region. We will use this boundary condition in Sec. IV to derive the nonlinear integral equation for the electric field on the surface of the substrate. This integral equation is then reduced to a system of coupled, nonlinear, algebraic equations with the aid of the method of moments. In Sec. V we discuss the numerical solution of this nonlinear system of equations in different scattering regimes, in particular, the regime when optical bistability is present. We also present numerical results that illustrate modification of the enhanced backscattering phenomenon due to nonlinear effects. Finally, in Sec. VI we present the conclusion drawn from the results obtained in this work.

II. FORMULATION OF THE SCATTERING PROBLEM: GEOMETRY AND BASIC EQUATIONS

The physical system we investigate is depicted in Fig. 1. It consists of vacuum in the region $x_3 > \zeta(x_1) + D$ (region I), a nonlinear semiconductor film in the region $\zeta(x_1) + D > x_3 > \zeta(x_1)$ (region II), and a linear dielectric substrate in the region $x_3 < \zeta(x_1)$ (region III). The surface profile function $\zeta(x_1)$ is assumed to be a single-valued function of x_1, that is a stationary Gaussian process defined by the properties $\langle \zeta(x_1) \rangle = 0$ and $\langle \zeta(x_1)\zeta(x_1') \rangle = \delta^2 W(|x_1 - x_1'|)$, where the angle brackets denote an average over the ensemble of realizations of the surface profile and $\delta = \sqrt{\langle \zeta^2(x_1) \rangle}$ is the rms height of the surface. The surface height autocorrelation function is assumed to be given by $W(|x_1|) = \exp(-x_1^2/a^2)$, where a is the transverse correlation length of the surface roughness.

We consider the steady-state scattering of monochromatic light, and assume the time dependence of the electric field of the form $\boldsymbol{E}(\boldsymbol{x};t) = \boldsymbol{E}(\boldsymbol{x})\exp(-i\omega t)$, where $\boldsymbol{x} = (x_1, x_2, x_3)$ is the position vector and t is time. We suppress the dependence on ω in $\boldsymbol{E}(\boldsymbol{x})$ since no other frequencies are present.

We model the steady-state material response of the nonlinear semiconductor film by introducing the nonlinear dielectric function

$$\varepsilon_f(\omega;|\boldsymbol{E}|^2) = \varepsilon_\infty \frac{\omega_L^2 - \omega^2 - i\omega\gamma - \alpha(\omega)|\boldsymbol{E}|^2}{\omega_T^2 - \omega^2 - i\omega\gamma - \alpha(\omega)|\boldsymbol{E}|^2}, \qquad (1)$$

which depends on the frequency ω and the local intensity $|\boldsymbol{E}^{\mathrm{II}}(\boldsymbol{x})|^2$ of the field in the film. In Eq. (1) ε_∞ is the optical frequency dielectric constant, ω_T is the frequency of the transverse exciton of infinite wavelength, ω_L is the frequency of the longitudinal exciton of infinite wavelength, γ is the damping rate of the transverse excitonic modes, and $\alpha(\omega)$ is the frequency-dependent nonlinear parameter. An example of a material whose dielectric properties can be described by the function (1) is AlGaAs [22]. The substrate is described by a linear, real, and positive dielectric function $\varepsilon(\omega)$.

We will study the scattering of an s-polarized electromagnetic field, since the enhanced backscattering effect is more pronounced in s polarization than in p polarization in the scattering from dielectric substrates [23]. The plane of incidence for s-polarized light is the x_1x_3 plane and the only,

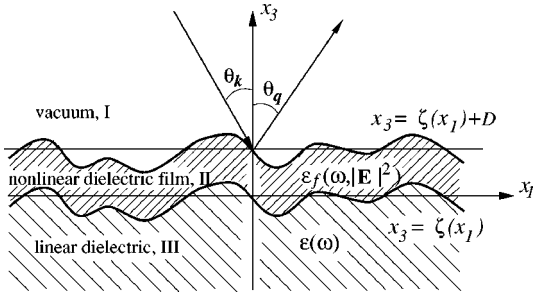

FIG. 1. Scattering geometry.

nonzero Cartesian component of the electric field is perpendicular to the plane of incidence and satisfies the equations

$$\left[\frac{\partial^2}{\partial x_1^2}+\frac{\partial^2}{\partial x_3^2}+\frac{\omega^2}{c^2}\right]E_2^{\mathrm{I}}(x_1,x_3)=0, \quad x_3>\zeta(x_1)+D \tag{2a}$$

$$\left[\frac{\partial^2}{\partial x_1^2}+\frac{\partial^2}{\partial x_3^2}+\varepsilon_f(\omega,|E_2^{\mathrm{II}}|^2)\frac{\omega^2}{c^2}\right]E_2^{\mathrm{II}}(x_1,x_3)=0,$$

$$\zeta(x_1)+D>x_3>\zeta(x_1) \tag{2b}$$

$$\left[\frac{\partial^2}{\partial x_1^2}+\frac{\partial^2}{\partial x_3^2}+\varepsilon(\omega)\frac{\omega^2}{c^2}\right]E_2^{\mathrm{III}}(x_1,x_3)=0, \quad x_3<\zeta(x_1) \tag{2c}$$

together with the boundary conditions that the field and its normal derivative are continuous across the interfaces,

$$E_2^{\mathrm{I}}(x_1,\zeta(x_1)+D)=E_2^{\mathrm{II}}(x_1,\zeta(x_1)+D), \tag{3a}$$

$$E_2^{\mathrm{II}}(x_1,\zeta(x_1))=E_2^{\mathrm{III}}(x_1,\zeta(x_1)), \tag{3b}$$

$$\left[-\zeta'(x_1)\frac{\partial}{\partial x_1}+\frac{\partial}{\partial x_3}\right]E_2^{\mathrm{I}}(x_1,x_3)|_{x_3=\zeta(x_1)+D}$$

$$=\left[-\zeta'(x_1)\frac{\partial}{\partial x_1}+\frac{\partial}{\partial x_3}\right]E_2^{\mathrm{II}}(x_1,x_3)|_{x_3=\zeta(x_1)+D}, \tag{3c}$$

$$\left[-\zeta'(x_1)\frac{\partial}{\partial x_1}+\frac{\partial}{\partial x_3}\right]E_2^{\mathrm{II}}(x_1,x_3)|_{x_3=\zeta(x_1)}$$

$$=\left[-\zeta'(x_1)\frac{\partial}{\partial x_1}+\frac{\partial}{\partial x_3}\right]E_2^{\mathrm{III}}(x_1,x_3)|_{x_3=\zeta(x_1)}. \tag{3d}$$

We assume that the scattering system is illuminated from the vacuum side by a plane wave, described by the electric field

$$E_2^{\mathrm{I}}(x_1,x_3)_{\mathrm{inc}}=A\exp\{i(\omega/c)(x_1\sin\theta_{\boldsymbol{k}}-x_3\cos\theta_{\boldsymbol{k}})\}, \tag{4}$$

where the constant A is the real amplitude of the incident wave and $\theta_{\boldsymbol{k}}$ is the angle of incidence. The magnitude of the total, time-averaged incident flux P_{inc} is given by

$$P_{\mathrm{inc}}=L_1L_2\frac{cA^2}{8\pi}\cos\theta_{\boldsymbol{k}}, \tag{5}$$

where L_1 and L_2 are the lengths of the surface in the x_1 and x_2 directions, respectively.

To find the far-field scattered intensity in the vacuum, up to a certain point we can follow the route developed in the linear theory [24]. Namely, we apply Green's second integral identity to region I to obtain the time-averaged incident flux scattered into an angular interval $d\theta_{\boldsymbol{q}}$ about the scattering direction defined by the angle $\theta_{\boldsymbol{q}}$:

$$P_{\mathrm{sc}}(\theta_{\boldsymbol{k}},\theta_{\boldsymbol{q}})=L_2\frac{c^2}{64\pi^2\omega}|r(\theta_{\boldsymbol{k}},\theta_{\boldsymbol{q}})|^2, \tag{6}$$

where the scattering amplitude $r(\theta_{\boldsymbol{q}},\theta_{\boldsymbol{k}})$ is given by

$$r(\theta_{\boldsymbol{q}},\theta_{\boldsymbol{k}})=\int_{-\infty}^{\infty}dx_1\,\exp\left\{-i\frac{\omega}{c}\{x_1\sin\theta_{\boldsymbol{q}}+[\zeta(x_1)+D]\cos\theta_{\boldsymbol{q}}\}\right\}$$

$$\times\left[i\frac{\omega}{c}[\zeta'(x_1)\sin\theta_{\boldsymbol{q}}-\cos\theta_{\boldsymbol{q}}]E^{\mathrm{I}}(x_1)-F^{\mathrm{I}}(x_1)\right]. \tag{7}$$

The dependence of $r(\theta_{\boldsymbol{k}},\theta_{\boldsymbol{q}})$ on the angle of incidence $\theta_{\boldsymbol{k}}$ is implicit, through the source functions

$$E^I(x_1)\equiv E_2^I(x_1,\zeta(x_1)+D), \tag{8a}$$

$$F^{\mathrm{I}}(x_1)\equiv\left[-\zeta'(x_1)\frac{\partial}{\partial x_1}+\frac{\partial}{\partial x_3}\right]E_2^{\mathrm{I}}(x_1,x_3)|_{x_3=\zeta(x_1)+D}. \tag{8b}$$

We characterize the scattered intensity by the average of the differential reflection coefficient (DRC), which gives the fraction of the total energy incident onto the surface that is scattered into an angular interval $d\theta_{\boldsymbol{q}}$ about $\theta_{\boldsymbol{q}}$:

$$\langle\partial R/\partial\theta_{\boldsymbol{q}}\rangle=\langle P_{\mathrm{sc}}(\theta_{\boldsymbol{k}},\theta_{\boldsymbol{q}})/P_{\mathrm{inc}}\rangle. \tag{9}$$

In the absence of the nonlinear film, this function is known [23] to display an enhanced backscattering peak, associated with the diffuse component of the scattered light, and appearing due to the constructive interference of multiply scattered waves provided the roughness parameters δ and a are of the order of the wavelength $\lambda=2\pi/c$.

With the aid of Eq. (5) and Eq. (6) we rewrite Eq. (9) as

$$\langle\partial R/\partial\theta_{\boldsymbol{q}}\rangle=\left[\frac{8\pi\omega}{c}L_1A^2\cos\theta_{\boldsymbol{k}}\right]^{-1}\langle|r(\theta_{\boldsymbol{k}},\theta_{\boldsymbol{q}})|^2\rangle. \tag{10}$$

Therefore to calculate the mean DRC we need to calculate the source functions (8), which yield $r(\theta_{\boldsymbol{k}},\theta_{\boldsymbol{q}})$ through Eq. (7). To do that, we have to solve Eqs. (2) with the boundary conditions (3) for the incident field (4). Although the methods of solution of the linear problem for $E^{\mathrm{I}}(x_1)$ and $F^{\mathrm{I}}(x_1)$ are well developed at the present time, e.g., the method of moments [24,20], no nonlinear version of these methods has existed until now. In the next sections we develop a method that allows calculating the source functions in the case when the nonlinear film is so thin that nonlinear effects can be taken into account by an appropriate modification of the boundary conditions at the vacuum-linear dielectric interface.

III. NONLINEAR EFFECTIVE IMPEDANCE BOUNDARY CONDITION FOR THE ROUGH DIELECTRIC SURFACE COATED BY A THIN NONLINEAR FILM

Typically for nonlinear problems, it is hopeless to look for the general solution of the scattering problem formulated in the preceding section. Instead, one tries to specify the range of system parameters, in which most of the interesting physical phenomena are displayed and in which the general equa-

tions can be reduced to a more tractable form. This is the approach that will be taken here. We first assume that the film thickness D is small compared to the wavelength λ of the incident light. This will allow deriving nonlinear effective boundary conditions at $x_3=\zeta(x_1)$ that approximately relate the field and its normal derivative in the vacuum to their counterparts in the dielectric. Thus one will be able to write the general solution for the field everywhere, since the bulk nonlinear medium will be excluded from the problem. Second, we consider a physically interesting frequency region around the frequency ω_T of the excitonic resonance in the film, so that the reflecting and absorbing properties of the surface become very sensitive to the amplitude of the incident field and the resulting field distribution on the rough surface. Finally, we assume that the magnitude of the imaginary optical skin depth $d=(c/\omega)[-\varepsilon(\omega)]^{-1/2}$ of the substrate is small compared to λ. This assumption allows writing an approximate local relation [23] between the electric field and its normal derivative in region III, evaluated at $x_3=\zeta(x_1)-D$,

$$\left[-\zeta'(x_1)\frac{\partial}{\partial x_1}+\frac{\partial}{\partial x_3}\right]E_2^{\mathrm{III}}(x_1,x_3)\big|_{x_3=\zeta(x_1)} =K(x_1)E_2^{\mathrm{III}}(x_1,x_3)\big|_{x_3=\zeta(x_1)}, \tag{11}$$

where

$$K(x_1)\cong\frac{\phi(x_1)}{d}\left[1+\frac{d}{2}\frac{\zeta''(x_1)}{\phi^3(x_1)}-\frac{d^2}{8}\frac{[\zeta''(x_1)]^2}{\phi^6(x_1)}\right] \tag{12}$$

is the local surface impedance and $\phi(x_1)=\{1+[\zeta'(x_1)]^2\}^{1/2}$. This last assumption is not very essential in our analysis (unlike the first one), but is very useful since it halves the number of equations to be solved numerically and saves a great deal of computer time. The utility of the impedance boundary condition (11) in computer simulation studies of the scattering of light from randomly rough linear dielectric surfaces was demonstrated by Maradudin and Méndez [23].

We will now show that in the case of a thin nonlinear film one can simplify the system of equations (2) with the boundary conditions (3) considerably. Namely, we will reduce the problem to the solution of just two equations in the regions $x_3>\zeta(x_1)$ (vacuum) and $x_3<\zeta(x_1)$ (linear dielectric), and two effective boundary conditions that take into account the influence of the thin nonlinear film. We will then further simplify the problem by using the impedance approximation. The method of effective boundary conditions proves to be very useful for linear electromagnetic problems where thin films are present [25], although it has not yet been used in the context of scattering from rough films. Here we develop this method for the scattering of light from a randomly rough, thin, nonlinear film deposited on a linear substrate.

Assuming that the electric field inside the film changes little in the x_3 direction, we expand both sides of Eq. (3c) in the vicinity of $x_3=\zeta(x_1)$ to first order in D:

$$\left[-\zeta'(x_1)\frac{\partial}{\partial x_1}+\frac{\partial}{\partial x_3}\right][E_2^{\mathrm{I}}-E_2^{\mathrm{II}}]\big|_{x_3=\zeta(x_1)} =-D\left[\frac{\partial^2}{\partial x_1\partial x_3}+\frac{\partial^2}{\partial x_3^2}\right][E_2^{\mathrm{I}}-E_2^{\mathrm{II}}]\big|_{x_3=\zeta(x_1)}. \tag{13}$$

Since we seek an approximate relation between E_2^{I} and E_2^{III} at $x_3=\zeta(x_1)$, we use Eq. (3d) in the left hand side of Eq. (13) and replace E_2^{II} by E_2^{III}. Then, we notice that

$$\zeta'(x_1)\frac{\partial}{\partial x_3}=\left\{\frac{\partial}{\partial x_1}+\zeta'(x_1)\frac{\partial}{\partial x_3}\right\}-\frac{\partial}{\partial x_1},$$

where the term in the curly brackets is the tangential derivative. Since tangential derivative of the field is continuous across the interfaces, we obtain to first order in D

$$\left[-\zeta'(x_1)\frac{\partial}{\partial x_1}+\frac{\partial}{\partial x_3}\right][E_2^{\mathrm{I}}-E_2^{\mathrm{III}}]\big|_{x_3=\zeta(x_1)} =-D\left[\frac{\partial^2}{\partial x_1^2}+\frac{\partial^2}{\partial x_3^2}\right][E_2^{\mathrm{I}}-E_2^{\mathrm{II}}]\big|_{x_3=\zeta(x_1)}. \tag{14}$$

We next use Eqs. (2a), (2b), and (3a) in the right hand side of Eq. (14), keeping only the terms of zeroth order in D in the fields, since the right hand side itself is already proportional to D, and obtain

$$\left[-\zeta'(x_1)\frac{\partial}{\partial x_1}+\frac{\partial}{\partial x_3}\right][E_2^{\mathrm{I}}-E_2^{\mathrm{III}}]\big|_{x_3=\zeta(x_1)} =D\frac{\omega^2}{c^2}[1-\varepsilon_f(\omega,|E_2^{\mathrm{I}}|^2)]E_2^{\mathrm{I}}\big|_{x_3=\zeta(x_1)}. \tag{15}$$

This is the first of the two effective boundary conditions. The second one is obtained by expanding both sides of Eq. (3a) in the vicinity of $x_3=\zeta(x_1)$,

$$E_2^{\mathrm{I}}\big|_{x_3=\zeta(x_1)}+D\frac{\partial}{\partial x_3}E_2^{\mathrm{I}}\big|_{x_3=\zeta(x_1)} =E_2^{\mathrm{II}}\big|_{x_3=\zeta(x_1)}+D\frac{\partial}{\partial x_3}E_2^{\mathrm{II}}\big|_{x_3=\zeta(x_1)}. \tag{16}$$

We notice that

$$\frac{\partial}{\partial x_3}\equiv\frac{1}{\phi(x_1)}\left[\frac{\partial}{\partial n}+\frac{\partial}{\partial\tau}\right], \tag{17}$$

where $\partial/\partial n$ and $\partial/\partial\tau$ are the normal and tangential derivatives on the surface $x_3=\zeta(x_1)$, respectively. Since both $\partial E_2/\partial n$ and $\partial E_2/\partial\tau$ are continuous across the interfaces for the s-polarized field, we have the following result correct to first order in D:

$$E_2^{\mathrm{I}}\big|_{x_3=\zeta(x_1)}=E_2^{\mathrm{III}}\big|_{x_3=\zeta(x_1)}. \tag{18}$$

This is the second effective boundary condition that connects the fields in the media I and III. Thus we have simplified the scattering problem, since we now need to solve only linear differential equations in regions I and III, and the nonlinear-

ity is present only in the effective boundary condition (15). We simplify the problem even more by using the impedance boundary condition (11) in Eqs. (15) and (18). As a result, we obtain a single, nonlinear effective impedance boundary condition for the electric field E_2^{I}:

$$\left[-\zeta'(x_1)\frac{\partial}{\partial x_1}+\frac{\partial}{\partial x_3}\right]E_2^{\mathrm{I}}|_{x_3=\zeta(x_1)} = K_{\mathrm{eff}}(x_1,|E_2^{\mathrm{I}}|^2)E_2^{\mathrm{I}}|_{x_3=\zeta(x_1)}, \tag{19}$$

where

$$K_{\mathrm{eff}}(x_1,|E_2^{\mathrm{I}}|^2)=K(x_1)+\frac{\omega^2}{c^2}\frac{D}{\phi(x_1)}[1-\varepsilon_f(\omega,|E_2^{\mathrm{I}}|^2)] \tag{20}$$

is the local nonlinear effective impedance, and the local linear impedance $K(x_1)$ is given by Eq. (12).

IV. METHOD OF MOMENTS

We will next employ the effective boundary condition (19) to obtain the nonlinear integral equation for $E_2(x_1,\zeta(x_1))$ — the source function that completely determines the scattered field in the vacuum. The standard way of deriving a closed system of integral equations for the field $E_2(x_1,x_3)$ and its normal derivative at the interface, developed in the linear theory [24], fails when the problem involves a bulk nonlinear medium. However, since in our formulation of the problem the nonlinearity now enters only through the effective boundary condition (19), the derivation can be done in the same way as in the linear case [24], with the result

$$E(x_1)=E_2^{\mathrm{I}}(x_1,\zeta(x_1))_{\mathrm{inc}}+\int_{-\infty}^{\infty}dx_1'[H_0(x_1|x_1')E(x_1') - L_0(x_1|x_1')F(x_1')], \tag{21}$$

where the source functions $E(x_1)$ and $F(x_1)$ are now defined by

$$E(x_1)\equiv E_2^{\mathrm{I}}(x_1,\zeta(x_1)), \tag{22a}$$

$$F(x_1)\equiv\left[-\zeta'(x_1)\frac{\partial}{\partial x_1}+\frac{\partial}{\partial x_3}\right]E_2^{\mathrm{I}}(x_1,x_3)|_{x_3=\zeta(x_1)}, \tag{22b}$$

the kernels H_0 and L_0 are expressed in terms of the Hankel function of the first kind,

$$H_0(x_1|x_1')=\frac{i}{4}\left[-\zeta'(x_1)\frac{\partial}{\partial x_1'}+\frac{\partial}{\partial x_3'}\right]H_0^{(1)}\left\{\frac{\omega}{c}\{(x_1-x_1')^2+[\zeta(x_1)-x_3'+\eta]^2\}^{1/2}\right\}\Bigg|_{x_3=\zeta(x_1')}, \tag{23a}$$

$$L_0(x_1|x_1') = (i/4)H_0^{(1)}\left\{\frac{\omega}{c}\{(x_1-x_1')^2+[\zeta(x_1)-\zeta(x_1')+\eta]^2\}^{1/2}\right\}, \tag{23b}$$

and η is a positive infinitesimal. Using the effective boundary condition (19), we obtain a single integral equation for $E(x_1)$:

$$E(x_1)=E_2^{\mathrm{I}}(x_1,\zeta(x_1))_{\mathrm{inc}}+\int_{-\infty}^{\infty}dx_1'[H_0(x_1|x_1') - K_{\mathrm{eff}}(x_1,|E_2(x_1)|^2)L_0(x_1|x_1')]E(x_1'). \tag{24}$$

In the method of moments, we replace the infinite range of integration by the finite range $(-L/2,L/2)$ and divide the latter into N equal intervals. The functions in Eq. (24) are calculated at the midpoints of these intervals, $x_n=-L/2+(n-1/2)\Delta x$ $(n=1,2,3,\ldots,N)$, where $\Delta x=L/N$, as described by Maradudin and Méndez for the linear problem corresponding in our case to $D=0$. The integral equation is then converted into the matrix equation,

$$E(x_m)=2E_2^{\mathrm{I}}(x_m,\zeta(x_m))_{\mathrm{inc}}+\sum_{n=1}^{N}M_{mn}(|E(x_n)|^2)E(x_n), \tag{25}$$

where

$$M_{mn}=\begin{cases}\Delta x\left(-\frac{i}{2}\right)\frac{\omega^2}{c^2}\frac{H_1^{(1)}((\omega/c)\{(x_m-x_n)^2+[\zeta(x_m)-\zeta(x_n)]^2\}^{1/2})}{(\omega/c)\{(x_m-x_n)^2+[\zeta(x_m)-\zeta(x_n)]^2\}^{1/2}} \\ \times\{(x_m-x_n)\zeta'(x_n)-[\zeta(x_m)-\zeta(x_n)]\}-\Delta x\left(\frac{i}{2}\right)K_{\mathrm{eff}}(x_n,|E(x_n)|^2) \\ \times H_0^{(1)}((\omega/c)\{(x_m-x_n)^2+[\zeta(x_m)-\zeta(x_n)]^2\}^{1/2}), \quad m\neq n & (26a) \\ \Delta x\frac{\zeta''(x_m)}{2\pi\phi^2(x_m)}-\Delta x\left(\frac{i}{2}\right)K_{\mathrm{eff}}(x_m,|E(x_m)|^2)H_0^{(1)}\left(\frac{\omega}{c}\frac{\phi(x_m)\Delta x}{2e}\right), \quad m=n. & (26b)\end{cases}$$

The remaining problem is to solve Eq. (25) for $E(x_m)$ for each realization of the surface profile $\zeta(x_1)$, which can be generated for given δ and a by standard algorithms [24]. The solution should be used to calculate the scattering amplitude $r(\theta_q,\theta_k)$, which is now written as

$$r(\theta_q,\theta_k)=\Delta x\sum_{m=1}^{N}\exp\left\{-i\frac{\omega}{c}[x_m\sin\theta_q+\zeta(x_m)\cos\theta_q]\right\}\times\left[i\frac{\omega}{c}[\zeta'(x_m)\sin\theta_q-\cos\theta_q]-K_{\rm eff}(x_m,|E(x_m)|^2)\right]E(x_m). \quad (27)$$

This procedure should be performed for a large number N_p of realizations of the surface profile to do the ensemble averaging in Eq. (10).

The numerical solution of the set of N equations (25) proves to be much more complicated than it is in the linear problem, that just requires the use of any standard linear matrix equation solver. Our numerical simulations of the few cases of physical interest, presented in the next section, indicate that the method for each scattering regime and strength of nonlinearity should be carefully and appropriately chosen. Methods which may work perfectly in some regimes fail in other cases, especially when multiple solutions are present.

V. NUMERICAL SOLUTION AND RESULTS

A. Dielectric properties of the AlGaAs/GaAs system

We first discuss the dielectric properties of the scattering system. In our numerical calculations we assume that the substrate is GaAs, whose dielectric constant ε is frequency independent. This assumption holds for the frequencies sufficiently higher than the frequency ω_L of the longitudinal exciton in GaAs, where $\varepsilon(\omega)$ is just given by its limiting value $\varepsilon_\infty=12.6$. We choose AlGaAs for the film, whose dielectric properties can be modeled by the resonant dielectric function (1). This choice of the scattering system is stimulated by the wide use of AlGaAs/GaAs structures in modern technology and experiment [22]. The properties of Eq. (1) for AlGaAs are characterized by $\varepsilon_\infty=12.6$, and the values of $\omega_L=12\,219.6\ \text{cm}^{-1}$ and $\omega_T=12\,219\ \text{cm}^{-1}$ that are very close to each other [26]. The values of the damping constant γ and nonlinear parameter $\alpha(\omega)$ can be regulated by changing the temperature of the system [22]. The characteristic value of γ for AlGaAs is very small, typically of the order of $10^{-5}\omega_T$, and this also makes the use of AlGaAs in studying resonant nonlinear phenomena very attractive.

We will adopt the convention of normalizing the amplitude of the electric field to the value E_0 that yields the typical experimental value [22] of the field intensity $(c/4\pi)E_0^2=10^4\ \text{W/cm}^2$. The typical value of the parameter $\alpha(\omega)$ in the vicinity of resonant frequency ω_T, estimated from the experimental data of Park *et al.* [22], is given by $\alpha E_0^2/\omega_T^2\approx 10^{-4}+i10^{-5}$. Note that the sign of the imaginary part can be positive or negative, depending on the frequency ω and the temperature of our system.

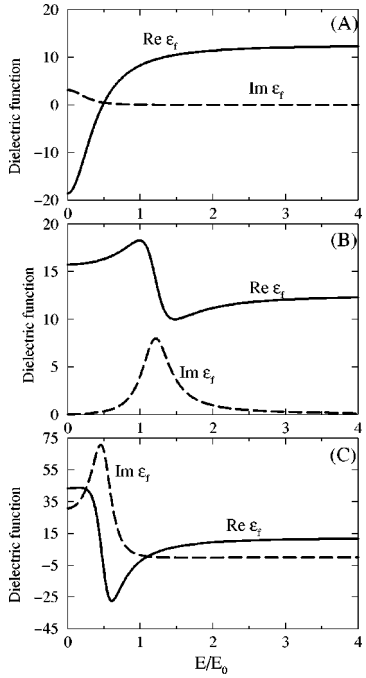

FIG. 2. Real and imaginary parts of the dielectric function $\varepsilon_f(\omega;|\boldsymbol{E}|^2)$ of the nonlinear AlGaAs film plotted versus the field amplitude E normalized to the characteristic amplitude E_0 at a fixed frequency ω: (A) $\omega=1.000\,01\omega_T$, (B) $\omega=0.99\,99\omega_T$, (C) $\omega=0.999\,99\omega_T$.

The behavior of $\varepsilon_f(\omega,|E|^2)$ as a function of $|E|^2$ for a fixed frequency can be very different depending on how close we are to ω_T and whether ω is above or below ω_T. We illustrate this variety by considering three values of ω, namely, $\omega=1.000\,01\omega_T$, $\omega=0.9999\omega_T$, and $\omega=0.999\,99\omega_T$, shown in Figs. 2(A) 2(B), and 2(C), respectively. One sees from these examples that different local field intensities can cause the film to behave like a metal, or like a dielectric, can cause very high absorption or almost no absorption. We now turn to the use of these three illustrative cases in our numerical solution of the scattering problem.

B. The use of iterative techniques in the study of the enhanced backscattering effect in the presence of nonlinearity

To investigate the role of nonlinearity in the multiple scattering of light, we assume the surface to be very rough, with parameters $\delta=1.6\ \mu$m and $a=2.65\ \mu$m, since the scattering of light whose frequency is near to ω_T from such a surface with no nonlinear film gives rise to a well-pronounced enhanced backscattering peak. We study the effect caused by the presence of an AlGaAs film of thickness $D=10$ nm, and first consider the scattering of s-polarized light of frequency $\omega=1.000\,01\omega_T$. The dielectric function of the film at this frequency, plotted versus the field amplitude, is shown in Fig. 2(A).

In the numerical solution of the nonlinear matrix equation (25) for $E(x_m)$ we applied the following algorithm. We started by taking a small amplitude of the incident field $A_{\rm min}=0.05E_0$ to ensure that the nonlinear term in the effective impedance (20) is negligible and solved the matrix equation (25) in the absence of the nonlinearity exactly, assuming the number of points on the surface to be $N=300$ and the

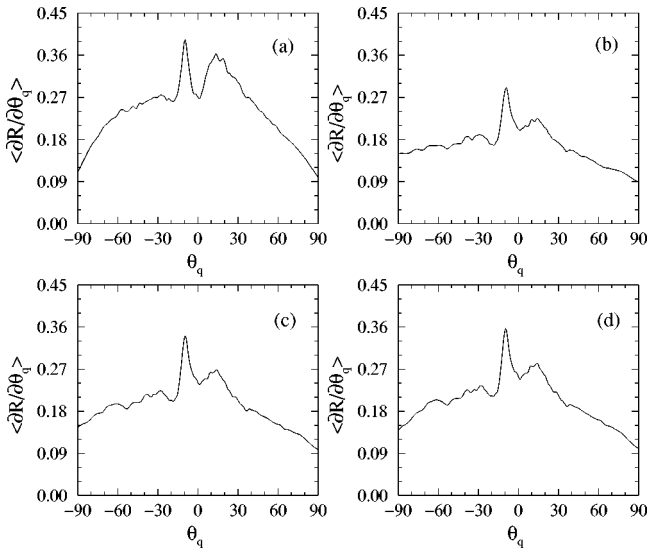

FIG. 3. Mean differential reflection for the light of frequency $\omega=1.000\,01\omega_T$ scattered from a system characterized by $\delta=1.6$ μm, $a=2.65$ μm, $D=100$ Å. The number of points on the surface is $N=300$ and the number of realizations is $N_p=2000$. The incident beam is described by the angle of incidence $\theta_k=10°$, and amplitude A, which is (a) $0.25E_0$, (b) $3E_0$, (c) $6E_0$, and (d) $9E_0$.

length of the surface along the x_1 direction to be $L=30$ μm. Then we increased the incident field amplitude A by the small step $\Delta A=0.05E_0$ and substituted the array $E(x_m)$ obtained at the preceding step into $K_{\text{eff}}(x_m,|E(x_m)|^2)$. We solved the resulting linear matrix equation for $E(x_m)$, used the solution to calculate $K_{\text{eff}}(x_m,|E(x_m)|^2)$, and repeated the iterations over and over until convergence was reached (usually no more than four iterations were needed to reach an accuracy of 2%). Only then did we increase the amplitude of the incident field A by the same small amount. For this new value of A we repeated the iteration procedure again, and continued increasing A up to the desired large value (in this case we took $A_{\max}=10E_0$, where the nonlinear response of the system reached saturation). For each value of A the calculated function $E(x_1)$ was used to find the other source function $F(x_1)$, with the aid of Eq. (19), and then both functions were used to calculate the scattering amplitude $r(\theta_q,\theta_k)$. We then repeated the same procedure, but now decreasing the amplitude A from $A_{\max}$ to $A_{\min}$ to see if any difference between the direct and reverse iterations existed due to possible hysteresis behavior, and found none. We were able to find thereby $r(\theta_q,\theta_k)$ for any amplitude A of the incident field for $N_p=2000$ realizations of the surface profile and to calculate the mean DRC from Eq. (10) by averaging the results over the ensemble of realizations of $\zeta(x_1)$ for each fixed A.

Figure 3 shows the mean DRC for four different amplitudes of the field incident at $\theta_k=10°$ on the scattering system. Nonzero values of the DRC at $\theta_k=\pm 90°$ appear due to the use of the effective boundary conditions, and correspond to the energy captured inside the film. We see that the height of the enhanced backscattering peak decreases as we increase A and then begins to increase until it saturates. This nonlinear effect, somewhat better illustrated in Fig. 4, showing $\langle \partial R/\partial\theta_q\rangle$ versus A for $\theta_q=-10°$ (retroreflection direction) and $\theta_q=30°$, can be explained as follows.

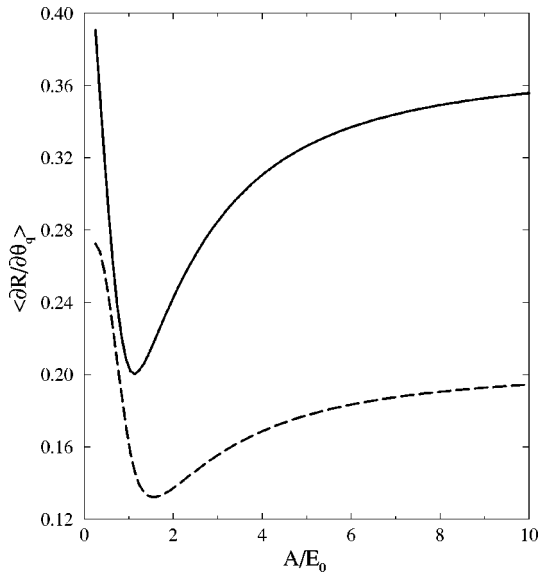

FIG. 4. Function $\langle \partial R/\partial\theta_q\rangle$ versus the amplitude of the incident field for fixed angles of incidence and scattering: $\theta_k=10°$, $\theta_q=-10°$ (solid line), and $\theta_q=30°$ (dashed line). The parameters of the system are the same as in Fig. 3 and $\omega=1.000\,01\omega_T$.

The behavior of $\varepsilon_f(\omega;|\boldsymbol{E}|^2)$ shown in Fig. 2(A) implies that the incident wave of low intensity ''sees'' essentially a thin metallic film deposited on a dielectric substrate. Conversely, the wave of high intensity effectively is likely to give rise to the field of high intensity in the film, and the effective dielectric constant of the film is close to ε_∞. The wave incident from the vacuum interacts more strongly with the medium whose optical density differs significantly from that of the vacuum. This is why the enhanced backscattering peak that occurs due to the constructive interference of the multiply scattered waves is known [24] to be most intense for metals with a large and negative dielectric constant or dielectrics with a large and positive dielectric constant. Therefore we expect the scattered intensity to have its maxima in the limits $A\to 0$ and $A\to\infty$, where A is the amplitude of the incident field. Figure 4 shows that the effect is most visible in the vicinity of the backscattering peak, which accumulates contributions from the waves that undergo several nonlinear interactions.

We next look at the scattering of light from the same system, but at the frequency $\omega=0.9999\omega_T$. Figure 2(B) illustrates the experimental fact that at the frequencies just below ω_T the absorption in AlGaAs becomes important. Neither very low nor very high A's can yield a field distribution inside the film that gives rise to noticeable absorption — only the intermediate values can. The computer simulation carried out by the iterative technique developed for the case (A) confirms this expectation. Figure 5, which presents $\langle \partial R/\partial\theta_q\rangle$ for $\theta_k=10°$, $\theta_q=-10°$ and $\theta_k=10°$, $\theta_q=30°$, demonstrates that the resonant absorption in the film suppresses the scattered intensity in the vacuum for intermediate values of A. Again, the effect is especially pronounced for the multiply scattered component of the scattered light.

Both cases considered above illustrate that nonlinear effects can lead to rather significant changes in the far-field scattered intensity. As long as there are no multiple solutions, the combination of a linear matrix equation solver with

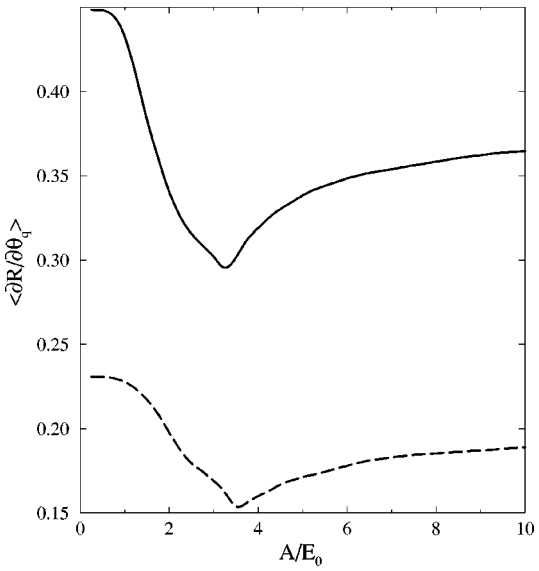

FIG. 5. Same as Fig. 4 but for $\omega = 0.9999\omega_T$.

an iterative technique described above gives a robust and efficient way of solving the scattering problem numerically.

C. Scattering from a rough surface in the presence of optical bistability. Kirchhoff approximation

We, finally, consider the case when Eq. (25) allows more than a single solution. To do this, we set the frequency very close to the resonance: $\omega = 0.999\,99\omega_T$. The dielectric function of the film at this frequency is shown in Fig. 2(C).

We first note that the film of AlGaAs with $D = 10$ nm, deposited on a GaAs substrate, gives a bistable response when there is no surface roughness ($\delta = 0$). The total field in the vacuum in this case can be written as

$$E_2^{\mathrm{I}}(x_1, x_3) = A\exp\{i(\omega/c)(x_1\sin\theta_{\boldsymbol{k}} - x_3\cos\theta_{\boldsymbol{k}})\} + AR_0(\theta_{\boldsymbol{k}}, |A|^2)\exp\{i(\omega/c)(x_1\sin\theta_{\boldsymbol{k}} + x_3\cos\theta_{\boldsymbol{k}})\}, \quad (28)$$

where the first term gives the incident field and the second term gives the reflected field and is defined by the intensity-dependent, complex Fresnel coefficient $R_0(\theta_{\boldsymbol{k}}, |A|^2)$. A straightforward solution for $R_0(\theta_{\boldsymbol{k}}, |A|^2)$ gives a curve that displays a non-single-valued dependence on A for all angles of incidence $\theta_{\boldsymbol{k}}$. In Fig. 6 we plot the reflectivity $|R_0(\theta_{\boldsymbol{k}}, |A|^2)|^2$ for the case of normal incidence, $\theta_{\boldsymbol{k}} = 0°$. This dependence has a characteristic bistable form (absent for the cases $\omega = 1.000\,01\omega_T$ and $\omega = 0.9999\omega_T$, by the way) with the unstable part shown by the dashed line.

The presence of optical bistability significantly hampers the numerical solution of the scattering problem. The iteration scheme described in the preceding subsection and other iteration techniques we tried showed either poor or no convergence. The use of more sophisticated numerical methods is impeded by the large number $N = 300$ of coupled nonlinear equations to be solved for at least 1000 realizations of the surface profile and for at least 20 values of the amplitude of the incident field.

To find out whether bistable response still exists in the presence of surface roughness, we apply the Kirchhoff approximation. In the linear case this approximation is known to be applicable only to smooth surfaces whose typical radius of curvature is greater than the wavelength of the incident light. In this approximation, the incident plane wave is reflected from a plane tangent to the surface at each point, according to Eq. (28). Omitting the details, which can be found in the paper by Sentenac and Maradudin [27] in the linear case, we point out the essential part peculiar to the nonlinear problem and caused by the non-single-valued Fresnel coefficient $R_0(\theta_{\boldsymbol{k}}, |A|^2)$ as a function of A. We solved this problem by defining two single-valued Fresnel coefficients, and the scattered fields associated with these coefficients: (i) ''forward,'' defined by the curve $ABCEF$ in Fig. 6, and (ii) ''backward,'' defined by the curve $FEDBA$ in Fig. 6.

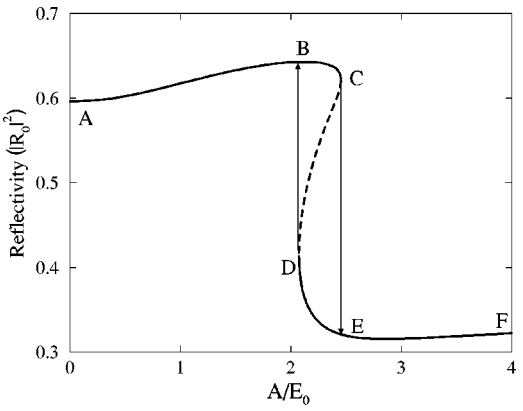

FIG. 6. Bistable reflectivity for planar ($\delta = 0$) film of thickness $D = 10$ nm at normal incidence and $\omega = 0.999\,99\omega_T$.

In our numerical simulations we assumed the roughness parameters to be given by $a = 4$ μm and $\delta = 0.5$ μm and 1 μm (the latter being on the edge of applicability of the Kirchhoff approximation). First of all, we checked the validity of the Kirchhoff approximation by substituting the values of $E(x_m)$ obtained into the original equation (25) and found that both the ''forward'' and ''backward'' solutions satisfied Eq. (25) quite well. Then we calculated the mean DRC for normal incidence and obtained that the hysteresis loop is observed in the entire range of the scattering angles. Several examples of this behavior are shown in Fig. 7. The comparison of the absolute values of the DRC shows the expected results: rougher surfaces produce the scattered intensity which is more uniformly distributed between the small and large scattering angles than it is in the case of less rough surfaces.

Thus the single-scattering component, calculated with the aid of the Kirchhoff approximation, displays the bistable effects existing in the reflection from the planar system. The question of the fate of optical bistability in the regime of strong multiple scattering has to be specially studied in the future. The most likely outcome, in our opinion, is the degradation of bistable effects since, for a very rough surface, the local responses of different parts of the surface can be very different, and the bistable effects can be washed out in the accumulated response.

VI. CONCLUSIONS

This paper presents, to our knowledge, the first quantitative investigation of the multiple scattering of light from the

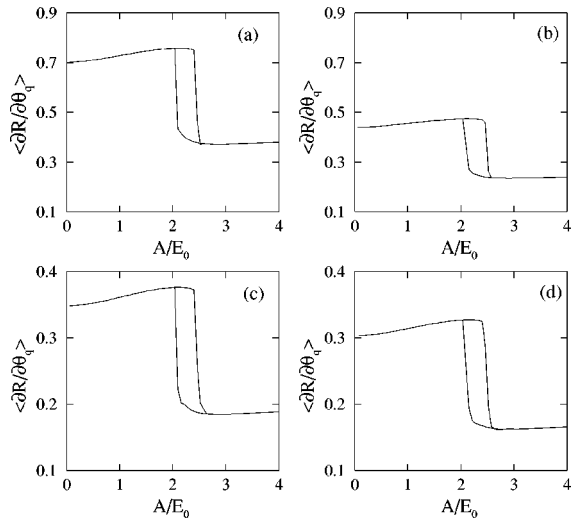

FIG. 7. Hysteresis loops in the scattered intensity at normal incidence: (a) $\delta=0.5$ μm, $a=4$ μm, $\theta_q=0°$; (b) $\delta=0.5$ μm, $a=4$ μm, $\theta_q=20°$; (c) $\delta=1$ μm, $a=4$ μm, $\theta_q=0°$; (d) $\delta=1$ μm, $a=4$ μm, $\theta_q=20°$. The frequency is $\omega=0.999\,99\omega_T$ and the thickness of the film is $D=10$ nm.

randomly rough surface of a nonlinear medium. The work was directed at the following as yet unstudied physical phenomena: (i) the coherent enhanced backscattering effect in rough surface scattering in the presence of nonlinearity, and (ii) bistability in reflection in the presence of random roughness. The theoretical investigation of such nonlinear scattering problems is always very difficult and cannot be treated by conventional ''linear'' methods, since it is impossible to write a general expression for the electromagnetic field in a nonlinear medium. The methods of deriving integral equations for the fields at the interfaces fail as long as one deals with a bulk nonlinear medium. Therefore additional, methodological, subjects of this work were (iii) the derivation of equations that give an adequate description of physical phenomena (i) and (ii), and have a form tractable to numerical analysis; and (iv) development of numerical algorithms for solving these equations.

We first showed that the nonlinear scattering problem is greatly simplified when the nonlinearity is localized in a thin layer near the surface — in our work this was modeled by the presence of a thin nonlinear film on the randomly rough surface of a semi-infinite linear substrate. We demonstrated that in the case when the film thickness is small compared to the wavelength of the incident light, the presence of a thin nonlinear film can be taken into account through nonlinear effective boundary conditions on the surface of a linear substrate. For the case of an s-polarized wave incident on the one-dimensional rough surface of a nonlinear film deposited on a substrate we derived these effective boundary conditions [Eqs. (15) and (18)]. Under the assumption that the substrate is significantly optically denser medium than the medium of incidence (vacuum), we used these boundary conditions to derive a single, nonlinear, impedance boundary condition for the electric field. Finally, with the aid of this boundary condition to obtain a single, nonlinear, integral equation (24) for the electric field on the surface of the substrate under the assumption that the substrate has a much larger dielectric constant than the incidence (vacuum).

A single nonlinear integral equation (24) is much easier to solve numerically than the nonlinear set of differential equations (2) for the field supplemented by the boundary conditions (3) and the incident field (4). As in the linear case [24], the method of moments reduces the integral equation to a closed set of algebraic equations (25), now nonlinear. Even so, different scattering regimes (defined by the strength of the random roughness and the strength of the nonlinearity) proved to require different algorithms to solve Eq. (25) numerically. As follows from our analysis in Sec. V, the combination of a linear matrix equation solver with iterative techniques provides a straightforward method of solving Eq. (25) as long as multiple solutions (bistability) are not present. Otherwise, approximate methods based on the Kirchhoff approximation can be helpful, although dealing with the multiple-scattering regime becomes very difficult in this case.

We chose the dielectric function of the nonlinear film in the resonant form (1) in preference to the traditionally assumed Kerr-like nonlinearity. This choice gives the possibility of changing the dielectric response of the film significantly by small changes of the frequency ω and the amplitude A of the incident wave when ω is close to the excitonic resonance frequency ω_T. If the surface is very rough and the enhanced backscattering peak is well pronounced in the far-field scattered intensity, we were able to obtain the modification of the angular distribution of the scattered intensity by nonlinear effects by an iterative technique. Such nonlinear phenomena as resonant absorption and changing the properties of the film from metallic to dielectric by increasing the amplitude of the incident field modify the angular intensity distribution, and their effect is especially well pronounced in the vicinity of the backscattering direction. This is explained by the fact that the enhanced backscattering peak occurs due to the constructive interference of waves scattered two or more times, which undergo more nonlinear interactions than singly scattered waves.

The case that proves to be the most difficult for numerical analysis is scattering in the presence of optical bistability. The nonlinear terms are by no means small here, and iterative schemes do not work. However, the use of the Kirchhoff approximation showed that the bistability in reflection from a planar system still exists in the scattering from a system with smoothly rough interfaces. The investigation of bistable effects in strongly multiple-scattering regimes will be a subject of future studies.

Thus we have investigated several aspects of the interplay between nonlinearity and disorder in rough surface scattering. Our results show that the presence of nonlinearity in the scattering of light from a random surface can lead to significant and interesting phenomena, and the variety of physically different scattering regimes gives an attractive opportunity for further theoretical and experimental work.

ACKNOWLEDGMENTS

This research was supported in part by Army Research Office Grant No. DAAH 04-96-1-0187. T. A. L. also acknowledges support from INTAS Grant No. 93-461.

[1] V. M. Agranovich and V. E. Kravtsov, Phys. Lett. A **131**, 378 (1988).
[2] V. E. Kravtsov, V. M. Agranovich, and K. I. Grigorishin, Phys. Rev. B **44**, 4931 (1991).
[3] V. M. Agranovich and V. E. Kravtsov, Phys. Lett. A **131**, 387 (1988).
[4] J. F. de Boer, A. Lagendijk, R. Sprik, and S. Feng, Phys. Rev. Lett. **71**, 3947 (1993).
[5] A. R. McGurn, T. A. Leskova, and V. M. Agranovich, Phys. Rev. B **44**, 11 441 (1991).
[6] X. Wang and H. J. Simon, Opt. Lett. **16**, 1475 (1991).
[7] H. J. Simon, Y. Wang, L. B. Zhou, and Z. Chen, Opt. Lett. **17**, 1268 (1992).
[8] O. A. Aktsipetrov, V. N. Golovkina, O. I. Kapusta, T. A. Leskova, and N. N. Novikova, Phys. Lett. A **170**, 231 (1992).
[9] Y. Wang and H. J. Simon, Phys. Rev. B **47**, 13 695 (1993).
[10] L. Kuang and H. J. Simon, Phys. Lett. A **197**, 257 (1995).
[11] K. A. O'Donnell, R. Torre, and C. S. West, Opt. Lett. **21**, 1738 (1996).
[12] K. A. O'Donnell, R. Torre, and C. S. West, Phys. Rev. B **55**, 7985 (1997).
[13] K. A. O'Donnell and R. Torre, Opt. Commun. **138**, 341 (1997).
[14] M. Leyva-Lucero, E. R. Méndez, T. A. Leskova, A. A. Maradudin, and Jun Q. Lu, Opt. Lett. **21**, 1809 (1996).
[15] A review of much of this work can be found in A. E. Kaplan, P. W. Smith, and W. J. Tomlinson, in *Nonlinear Surface Electromagnetic Waves*, edited by H.-E. Ponath and G. I. Stegeman (North-Holland, Amsterdam, 1991), p. 323.
[16] F. Bass and V. Freilikher, Waves Random Media **7**, 385 (1997).
[17] W. Chen and D. L. Mills, Phys. Rev. B **35**, 524 (1987).
[18] V. Freilikher, M. Pustilnik, and I. Yurkevich, Phys. Lett. A **193**, 467 (1994).
[19] T. A. Leskova, A. A. Maradudin, A. V. Shchegrov, and E. R. Méndez, Phys. Rev. Lett. **79**, 1010 (1997).
[20] J. Q. Lu, A. A. Maradudin, and T. Michel, J. Opt. Soc. Am. B **8**, 311 (1991).
[21] A. E. Danese, *Advanced Calculus, Vol. I* (Allyn and Bacon, Boston, 1965), p. 114.
[22] S. H. Park *et al.*, Appl. Phys. Lett. **52**, 1201 (1988).
[23] A. A. Maradudin and E. R. Méndez, Opt. Spektrosk. **80**, 459 (1996) [Opt. Spectrosc. **80**, 409 (1996)].
[24] A. A. Maradudin, T. Michel, A. R. McGurn, and E. R. Méndez, Ann. Phys. (N.Y.) **203**, 255 (1990).
[25] See, e.g., Appendix A in V. M. Agranovich and T. A. Leskova, Prog. Surf. Sci. **29**, 169 (1988).
[26] E. S. Koteles, in *Excitons*, edited by E. I. Rashba and M. D. Sturge (North-Holland, Amsterdam, 1982), p. 114.
[27] A. Sentenac and A. A. Maradudin, Waves Random Media **3**, 343 (1993).